Electronic Supplementary Material (ESI) for Dalton Transactions.

Supporting Information

Ultrafast Spectroscopy and Structural Characterization of a Photochromic Isomerizing Ruthenium Bis-sulfoxide Complex

Albert W. King,[†] *Jason P. Malizia,*[†] *James T. Engle,*[‡] *Christopher J. Ziegler*[‡] *and Jeffrey J. Rack*[*,†]

[†] Department of Chemistry and Biochemistry, Nanoscale and Quantum Phenomena Institute, Ohio University, Clippinger Laboratories, Athens, OH 45701 (USA)
[‡] Department of Chemistry, Knight Chemical Laboratory, University of Akron, Akron, OH 44325 (USA)

Structural Characterization

Similar to their respective thioether and sulfoxide analogues featuring an ethyl-bridged ligand, $[Ru(bpy)_2(bpte)]^{2+}$ (bpte is 1,2-bis(phenylthio)ethane)[1] and $[Ru(bpy)_2(bpSO)]^{2+}$, $[Ru(bpy)_2(bptp)]^{2+}$ and $[Ru(bpy)_2(bpSOp)]^{2+}$ appear to exhibit intramolecular π-stacking in the solid state. Such interactions are also observed in the structurally related $[Ru(phen)_2(bpte)]^{2+}$ (phen is 1,10-phenanthroline).[2] In $[Ru(bpy)_2(bptp)]^{2+}$, the distance between the centroid of the phenyl ring (atoms C21-C26, inclusive; bonded to S1) to the nearest bridgehead carbon (C15) of bpy is ~3.65 Å (see Figure 1 of the manuscript for numbering scheme). For the phenyl ring including C30-C35, bonded to S2, the distance to the nearest bridgehead bpy carbon (C5) is ~3.29 Å. The enantiomer exhibits phenyl-bpy distances of ~3.55 Å (phenyl C56-C61, bonded to S3, to bpy bridgehead C51) and 3.39 Å (phenyl C65-C70, bonded to S4, to bpy bridgehead C40). This stacking distance (phenyl C11-C16, bonded to S1, to bpy bridgehead C5) in $[Ru(bpy)_2(bpSOp)]^{2+}$ is ~3.43 Å. For comparison, the intramolecular distances reported for $[Ru(bpy)_2(bpte)]^{2+}$ are ~3.43 and ~3.98 Å, while those for $[Ru(bpy)_2(bpSO)]^{2+}$ are ~3.56 and ~3.48 Å. Indeed, while the shorter of the $[Ru(bpy)_2(bptp)]^{2+}$ intramolecular distances is considerably shorter than the reported distances in $[Ru(bpy)_2(bpte)]^{2+}$, the distances in $[Ru(bpy)_2(bpSOp)]^{2+}$ and $[Ru(bpy)_2(bpSO)]^{2+}$ are similar, suggesting that the observed π-stacking interactions is little affected by the extra atom in the chelate ring and that the impact of this intramolecular interaction will be comparable between the photochemistry of $[Ru(bpy)_2(bpSO)]^{2+}$ and $[Ru(bpy)_2(bpSOp)]^{2+}$.

Employing the Karplus equation to calculate dihedral angles based on J constants allows comparison between those derived from the crystal structure and the solution structure.[3] Spectral fitting in SpinWorks 3 was performed using a linewidth broadening of 4 Hz in order to adequately emulate the experimental data. In the case of the thioether complex, the calculated angles (from Sweet J, www.inmr.net) corresponding to the dihedral angles formed by atoms H_a-C64-C63-H_c, H_a-C64-C63-H_d, H_b-C64-C63-H_c and H_b-C64-C63-H_d are -46, -158, 60 and -41 °, respectively (See Figure 1 for labelling scheme). The corresponding angles observed in the crystal structure are -42.2(6), -157.3(5), 76.3(6) and -38.8(7) °, thus indicating fidelity between solution and solid state structures. The coupling constants describing the major species in the sulfoxide spectrum are similar to those of the thioether complex. The calculated dihedral angles based on the J constants from the NMR fit for H_a-C17-C18-H_c, H_a-C17-C18-H_d, H_b-C17-C18-H_c and H_b-C17-C18-H_d are -47, -153, 60 and -39 °, respectively. These angles are again consistent with those found in the solid state, where the corresponding angles were found to be -41.9(4), -157.7(3), 76.9(4) and -38.9(4) °. Calculated dihedral angles of the minor sulfoxide isomer indicate a dramatically different conformation in the propyl-bridge compared to the thioether complex. In this case, the dihedral angles for H_a-C17-C18-H_c, H_a-C17-C18-H_d, H_b-C17-C18-H_c and H_b-C17-C18-H_d are -4, -111, 110 and 0 °.

On Quantum Yield Calculations

Aggregate quantum yield of isomerization measurements were determined by irradiating solutions of the S,S-bonded complex in propylene carbonate or 1,2-dichloroethane at room temperature. An 0.800 mW UVTOP 365 nm UV LED was employed as the light source. Incident radiation intensity, I_0 (Equation 1), was determined using potassium ferrioxalate actinometry. In Equation 1, $\boldsymbol{n_{Fe^{2+}}}$ is moles of Fe^{2+} produced upon irradiation, Φ_λ is the quantum yield at the irradiation wavelength, t_i is the time in seconds the actinometer was irradiated and A_λ is the absorbance of the actinometer at the excitation wavelength during irradiation. Aggregate quantum yields of isomerization ($\Phi_{S,S\rightarrow PP}$) were calculated using Equation 2, where $[S,S]_0$ is the concentration of the S,S-bonded isomer at the start of the experiment, $[PP]_t$ is the concentration of photoproducts (both the S,O- and O,O-bonded isomers) at time t, V is the volume of the solution, t is irradiation time in seconds and A_{irr} is the absorbance of the solution at the irradiation wavelength at time t. Aggregate quantum yields of isomerization were calculated at times less than 180 seconds and averaged to yield the reported aggregate quantum yield of isomerization.

$$\boldsymbol{I_0 = \frac{n_{Fe^{2+}}}{\Phi_\lambda t_i (1 - 10^{-A_\lambda})}} \qquad \text{Equation 1}$$

$$\boldsymbol{\Phi_{S,S\rightarrow PP} = \frac{[S,S]_0 V[\ln([S,S]_0) - \ln([S,S]_0 - [PP]_t)]}{t I_0 (1 - 10^{A_{irr}})}} \qquad \text{Equation 2}$$

The concentration of photoproducts at time t, $[PP]_t$, was obtained by performing a multivariable linear regression, where the absorption spectrum at time t and the extinction coefficient of each isomer was used to determine concentration of the S,S-, S,O- and O,O-bonded isomers. Photolysis data were fit between 350 nm and 550 nm in the multiple variable linear regression calculation. The sum of the concentrations of the S,O- and O,O-bonded isomers was used to determine $[PP]_t$.

Table S1. Crystallographic Data for $[Ru(bpy)_2(bptp)](PF_6)_2$ and $[Ru(bpy)_2(bpSOp)](BF_4)_2$

	$[Ru(bpy)_2(bptp)](PF_6)_2$	$[Ru(bpy)_2(bpSOp)](BF_4)_2$
Emp. form	$C_{35}H_{32}F_{12}N_4P_2S_2Ru$	$C_{35}H_{32}B_2F_8N_4O_2S_2Ru$
Form. weight	963.78	879.46
Crystal system	Monoclinic	Orthorhombic
Space group	P2(1)	Fdd2
a (Å)	13.534(7)	18.280(9)
b (Å)	19.469(10)	42.77(3)
c (Å)	14.094(7)	9.005(5)
α (deg)	90	90
β (deg)	99.475(6)	90
γ (deg)	90	90
temperature (K)	100	100
wavelength (Å)	0.71073	0.71073
volume (Å)	3663(3)	7041(6)
space group	P2(1)	Fdd2
M_r	963.78	879.46
density (g cm^{-3})	1.748	1.659
Z	4	8
μ	0.725	0.647
F000	1936.0	3552.0
h,k,l max	16,23,16	21,50,10
N_{ref}	12771	3169
T_{min}, T_{max}	0.857, 0.931	0.810, 0.876
data completeness	1.88/0.97	1.87/1.00
θ (max)	25.180	25.21
R (reflections)	0.0412 (11941)	0.0231 (3115)
*w*R2 (reflections)	0.0917 (12771)	0.0592 (3169)
S	1.190	1.040
N_{par}	1009	245

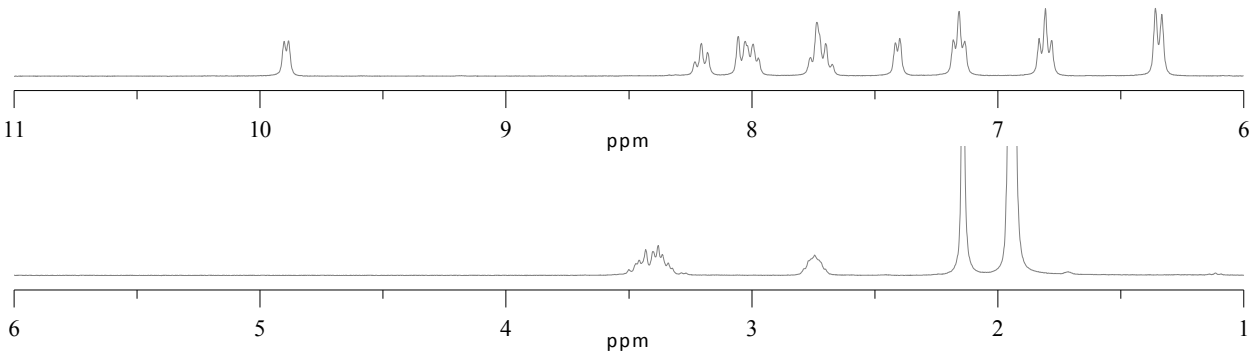

Figure S1. Proton NMR spectrum of $[Ru(bpy)_2(bptp)](PF_6)_2$ in d_3-acetonitrile. Peaks corresponding to the compound are at the following chemical shifts in ppm: 9.87 (d, 2 H), 8.19 (t, 2 H), 7.98 (m, 4 H), 7.68 (t, 4 H), 7.39 (d, 2 H), 7.14 (t, 4 H), 6.79 (t, 4 H), 6.33 (d, 4 H), 3.38 (m, 4 H), 2.73 (m, 2 H). Peaks at 2.13 and 1.94 correspond to water and residual acetonitrile, respectively.

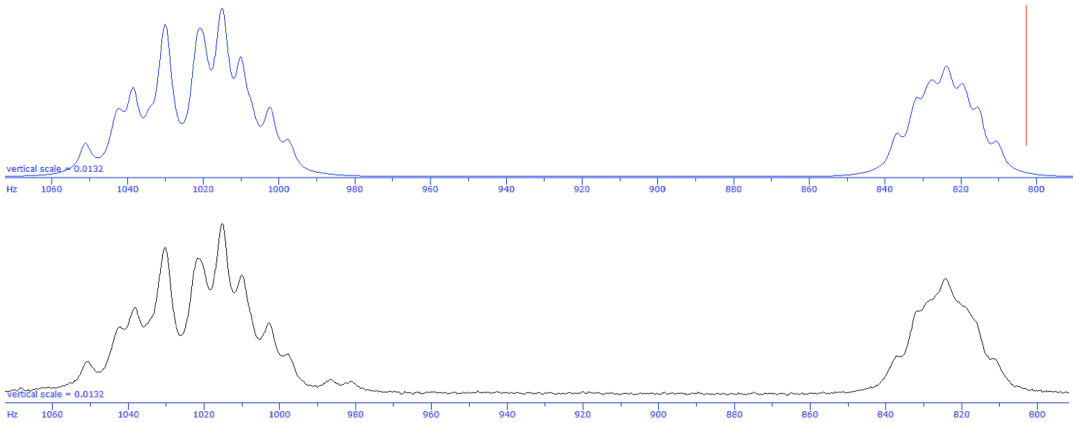

Figure S2. Simulated (above) and experimental (below) aliphatic NMR spectra of $[Ru(bpy)_2(bptp)]^{2+}$ in CD_3CN.

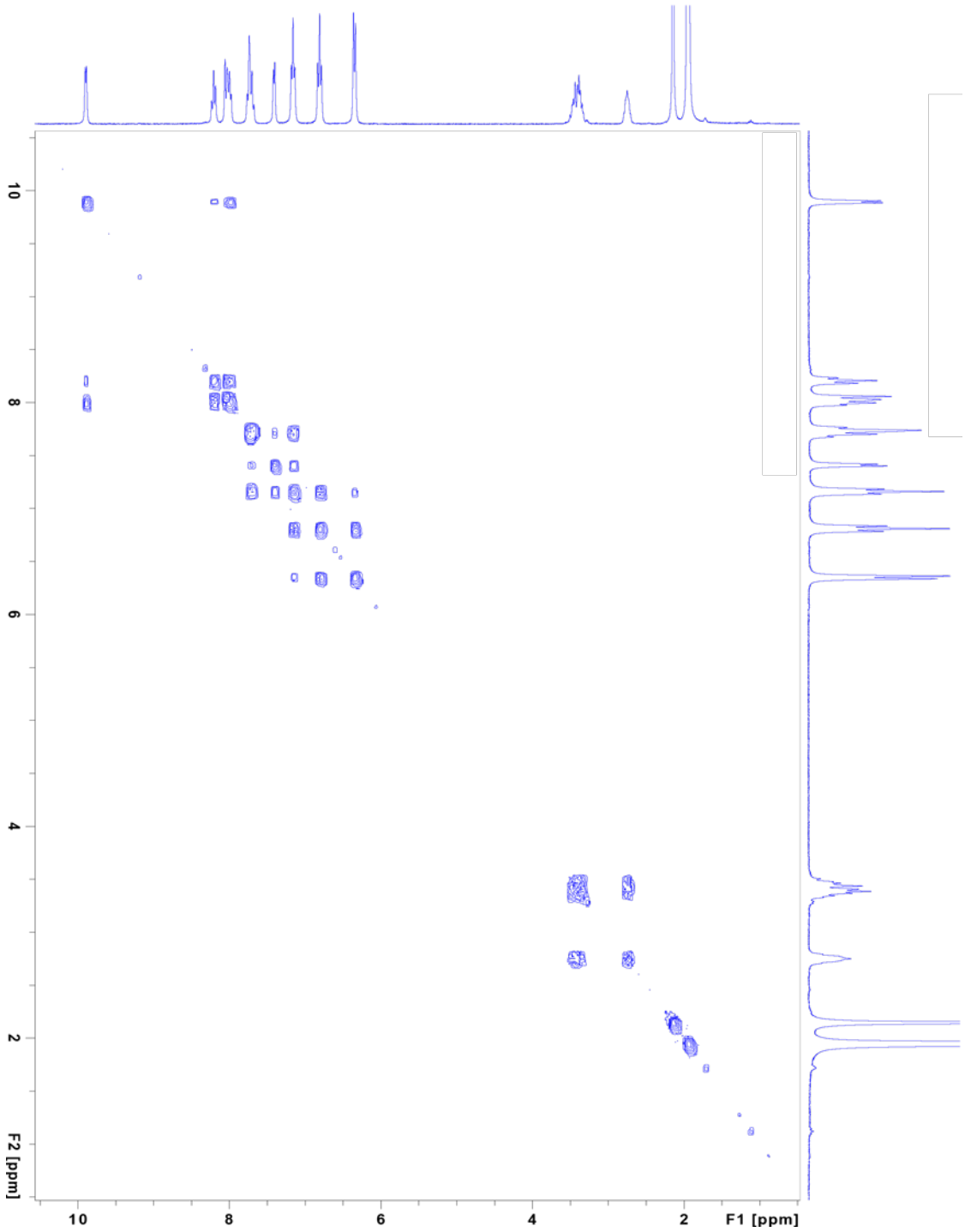

Figure S3. Correlation Spectroscopy (COSY) ^{1}H NMR spectrum of $[Ru(bpy)_2(bptp)](PF_6)_2$ in CD_3CN. The peak at 2.1 ppm is water.

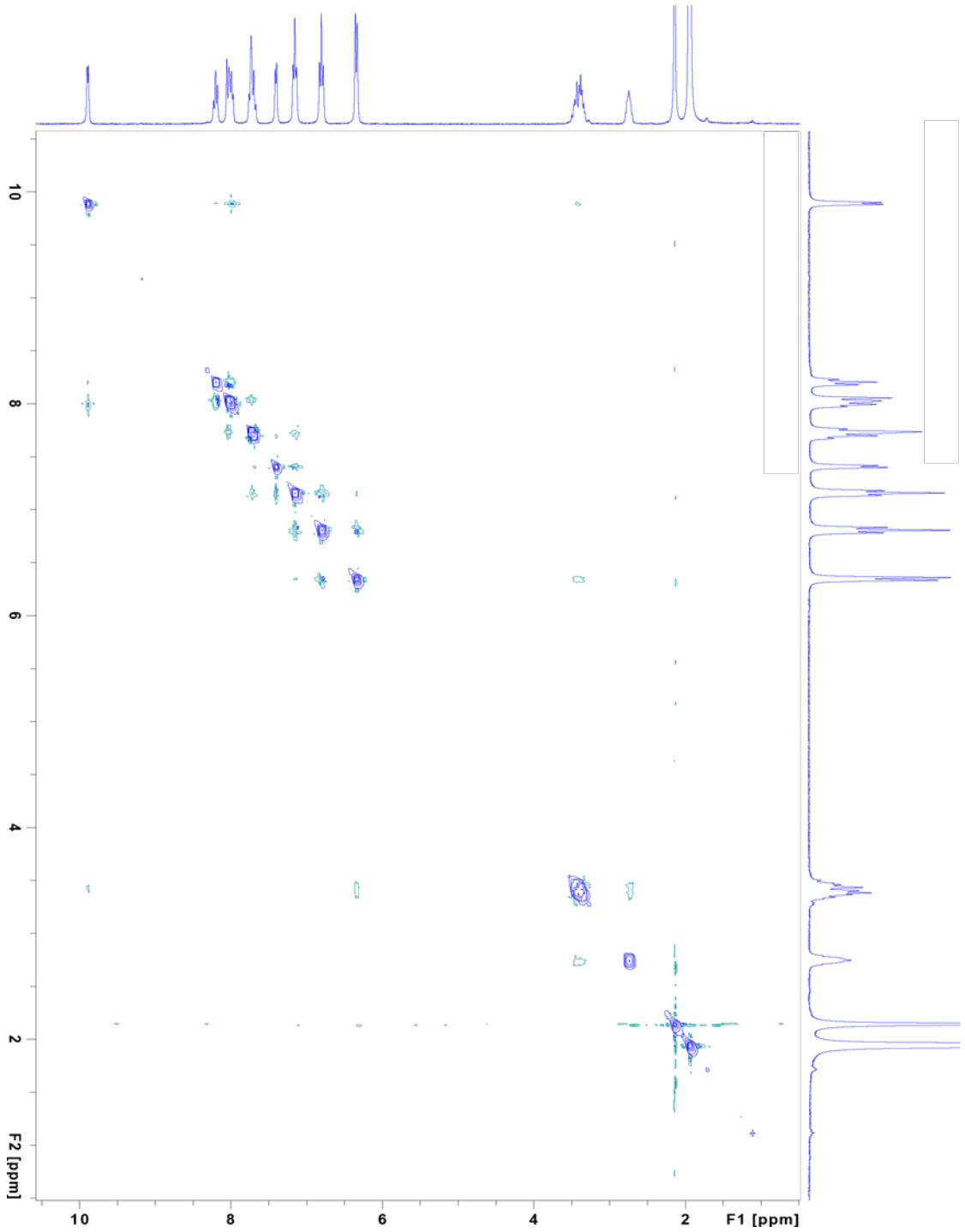

Figure S4. Nuclear Overhauser Spectroscopy (NOESY) ^{1}H NMR spectrum of $[Ru(bpy)_2(bptp)](PF_6)_2$ in CD_3CN. The peak at 2.1 ppm is water.

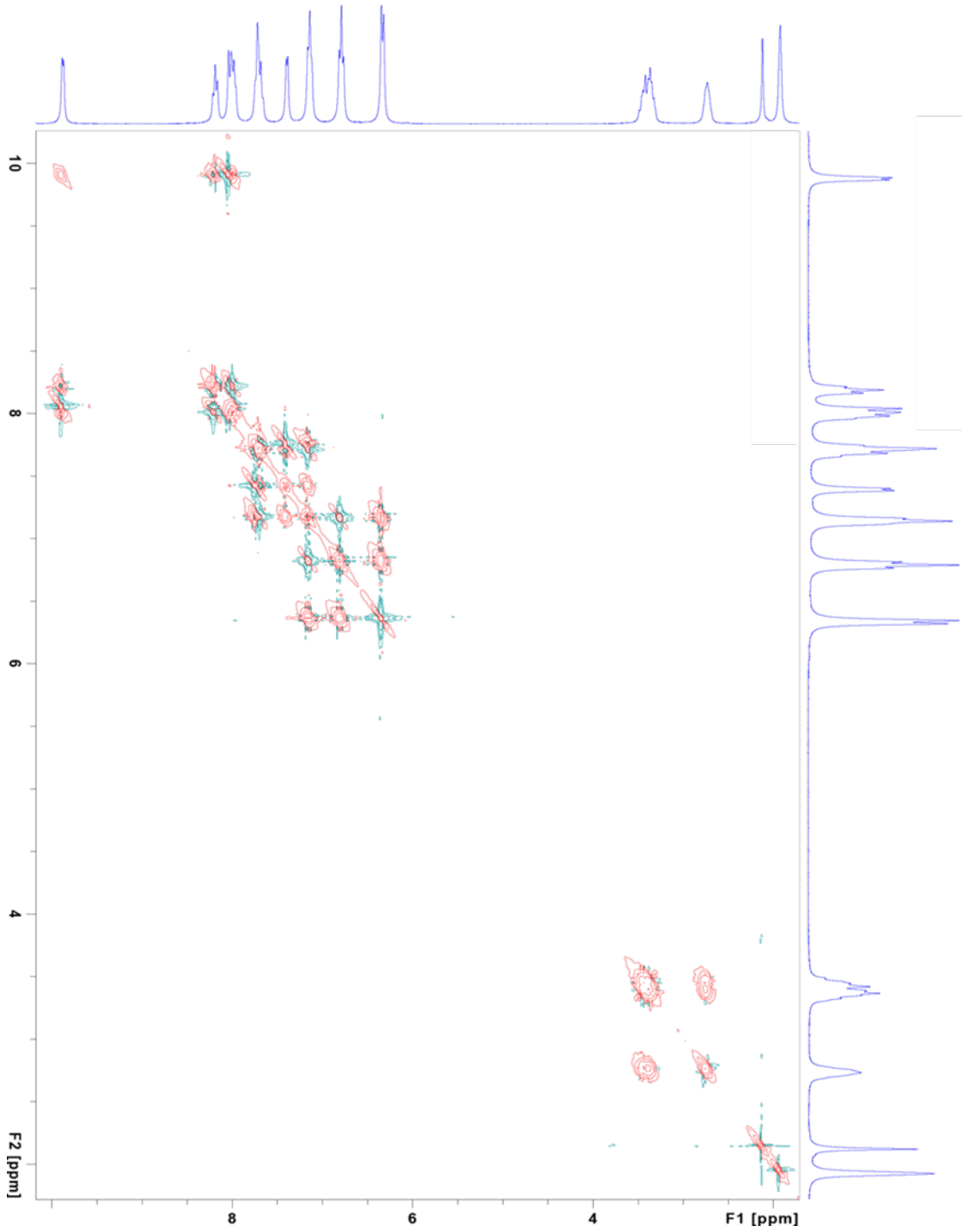

Figure S5. Total Correlation Spectroscopy (TOCSY) ^{1}H NMR spectrum of $[Ru(bpy)_2(bptp)](PF_6)_2$ in CD_3CN. The peak at 2.1 ppm is water.

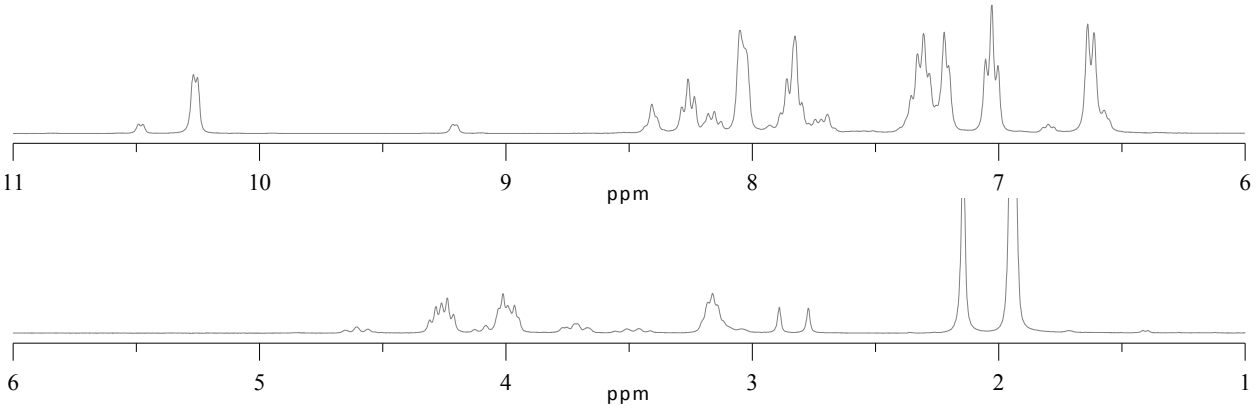

Figures S6. Proton NMR spectrum of $[Ru(bpy)_2(bpSOp)](PF_6)_2$ in d_3-acetonitrile. Peaks corresponding to the compound are at the following chemical shifts in ppm: 10.24 (d, 2 H), 8.24 (t, 2 H), 8.03 (d, 4 H) 7.81 (t, 4 H), 7.30 (m, 4 H), 7.22 (m, 2 H), 7.01 (t, 4 H), 6.59 (d, 4 H), 4.24 (m, 2 H), 3.97 (m, 2 H), 3.14 (m, 2 H). Peaks at 2.13 and 1.94 correspond to water and residual acetonitrile, respectively.

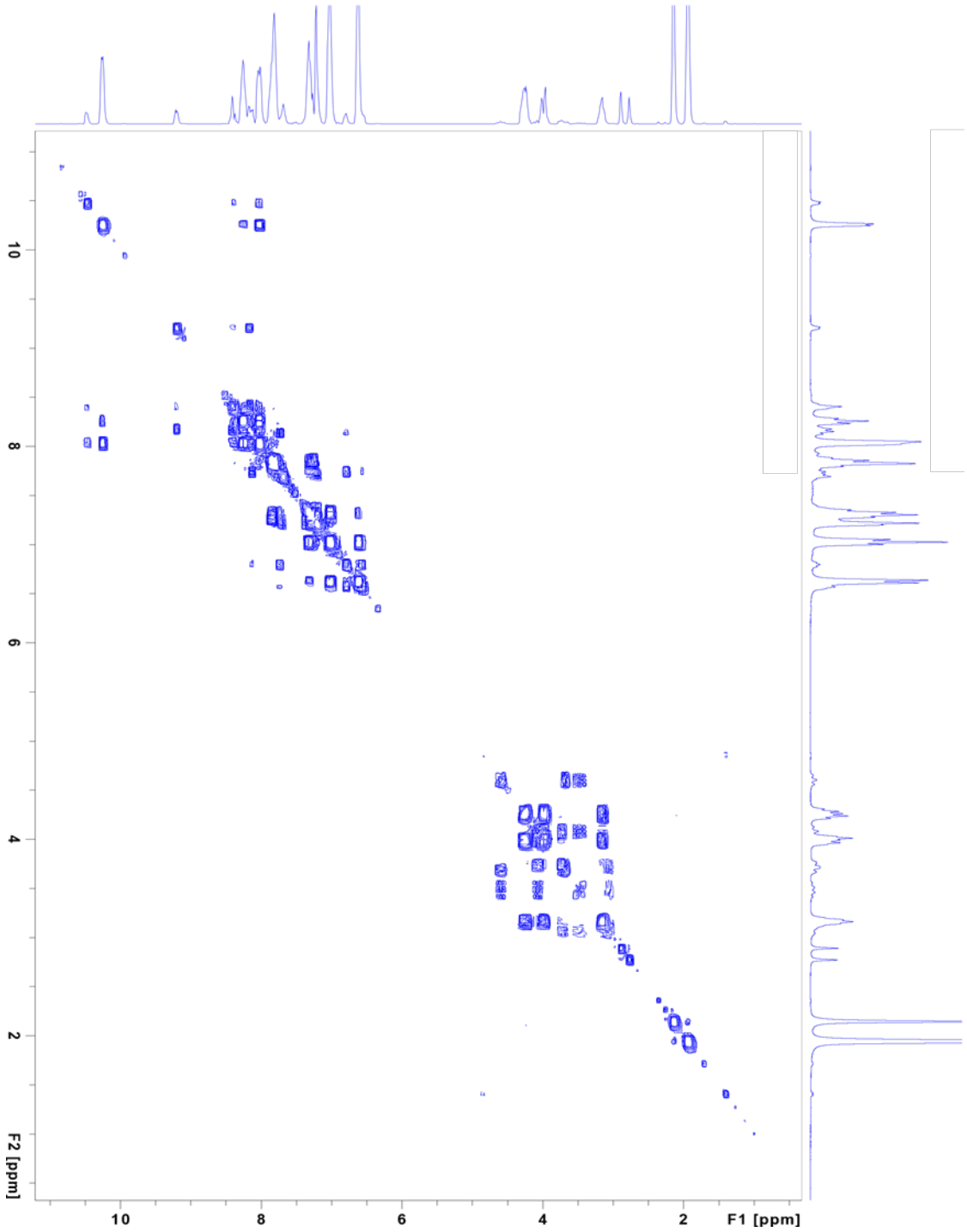

Figures S7. Correlation Spectroscopy (COSY) ^{1}H NMR spectrum of $[Ru(bpy)_2(bpSOp)](PF_6)_2$ in CD_3CN. The peak at 2.1 ppm is water.

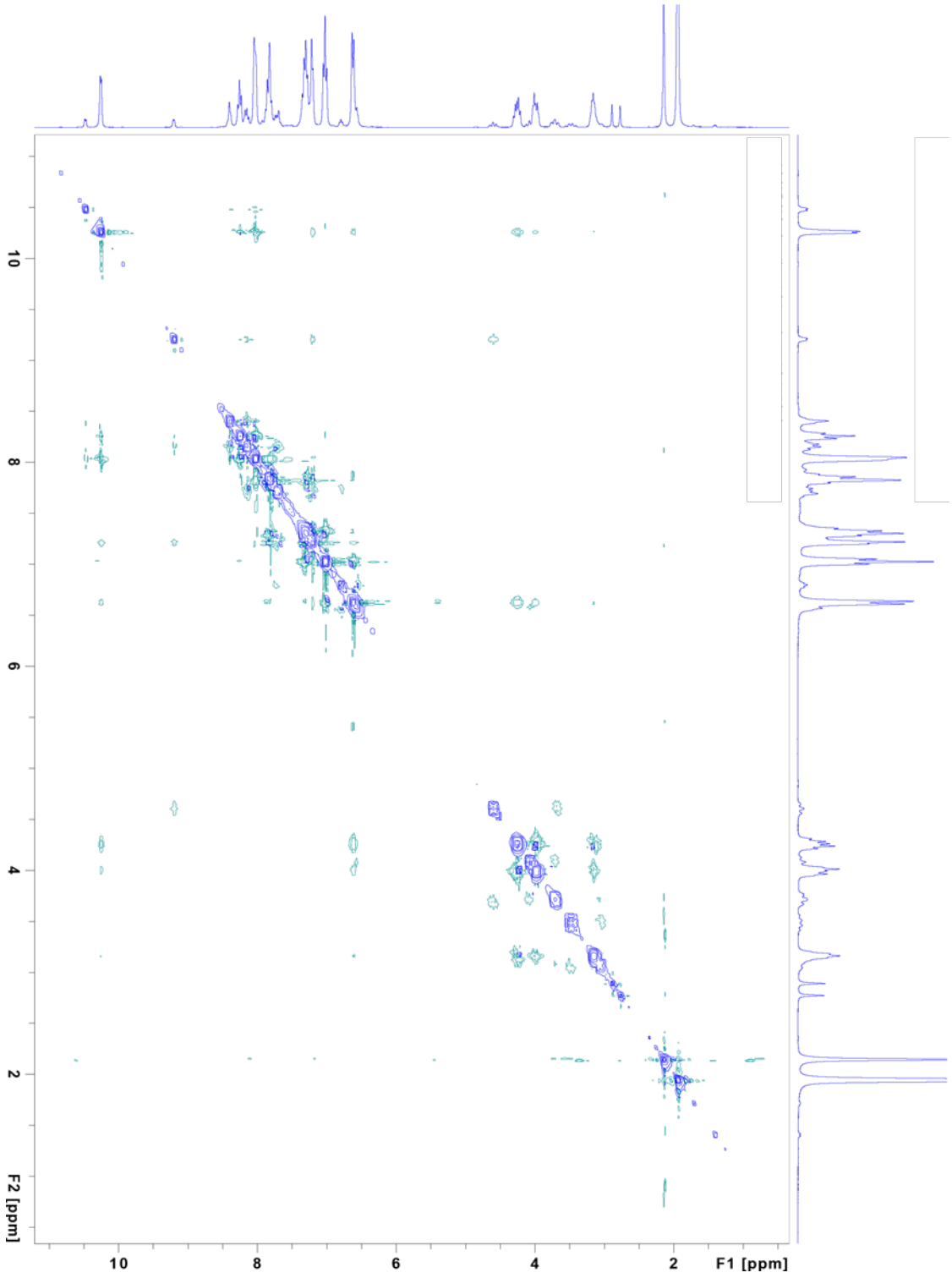

Figure S8. Nuclear Overhauser Spectroscopy (NOESY) ^{1}H NMR spectrum of $[Ru(bpy)_2(bpSOp)](PF_6)_2$ in CD_3CN. The peak at 2.1 ppm is water.

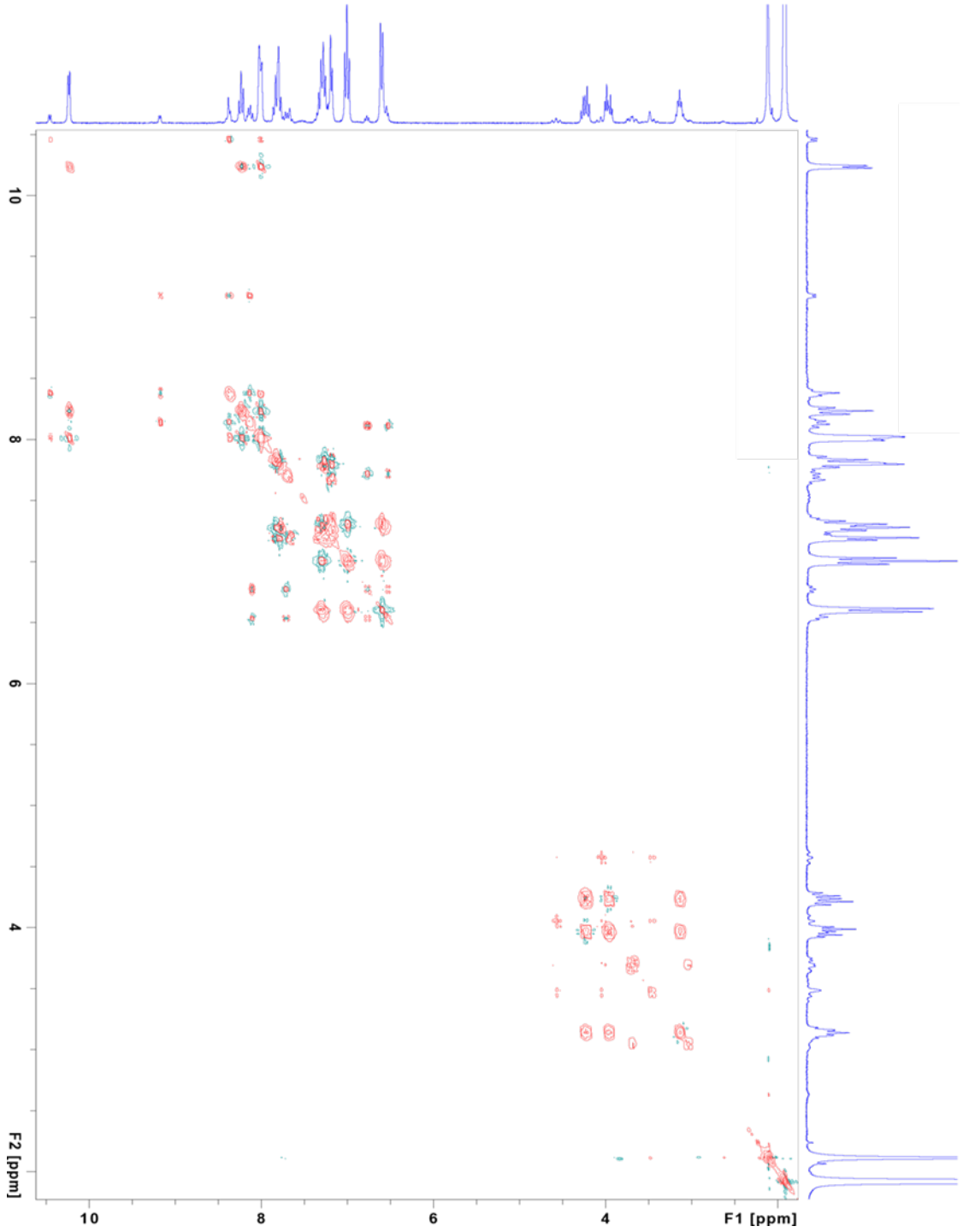

Figure S9. Total Correlation Spectroscopy (TOCSY) ^{1}H NMR spectrum of $[Ru(bpy)_2(bpSOp)](PF_6)_2$ in CD_3CN. The peak at 2.1 ppm is water.

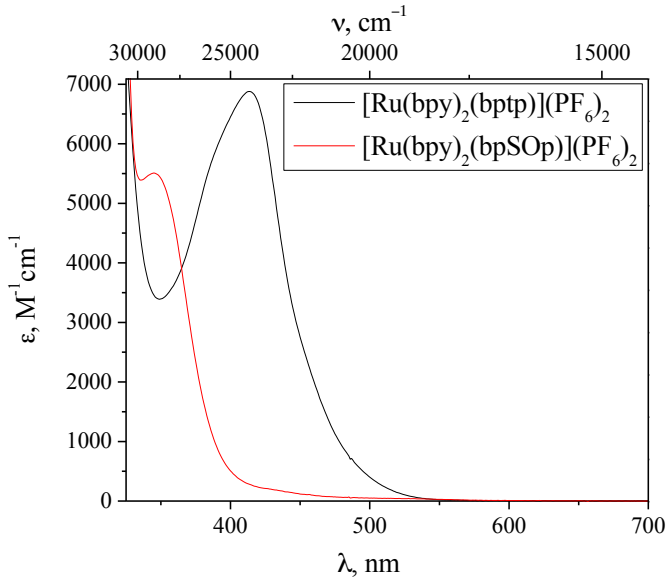

Figure S10. Electronic absorption extinction spectra of $[Ru(bpy)_2(bptp)](PF_6)_2$ (black) and $[Ru(bpy)_2(bpSOp)](PF_6)_2$ (red) in propylene carbonate.

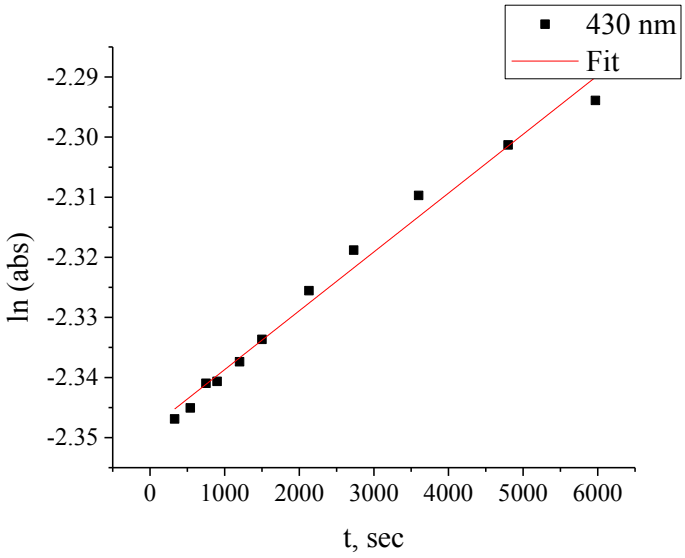

Figure S11. Thermal reversion kinetic trace of $[Ru(bpy)_2(bpSOp)](PF_6)_2$ in propylene carbonate at 430 nm.

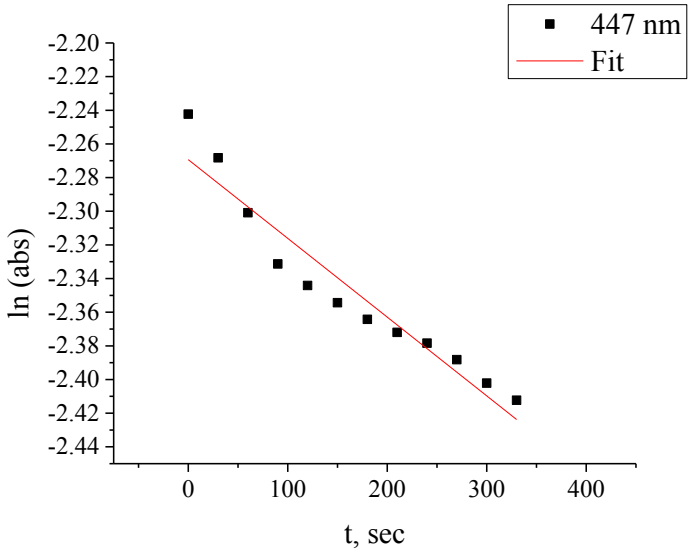

Figure S12. Thermal reversion kinetic trace of $[Ru(bpy)_2(bpSOp)](PF_6)_2$ in propylene carbonate at 447 nm.

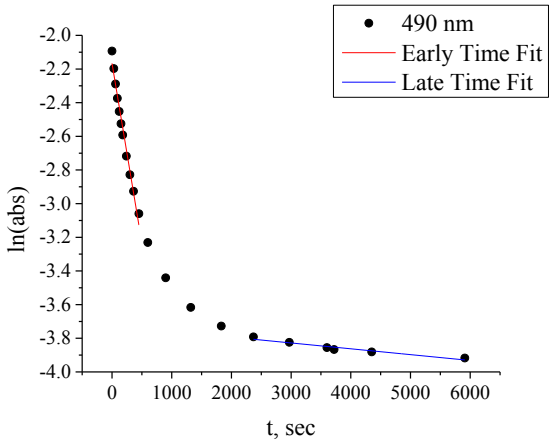

Figure S13. Thermal reversion kinetic trace of $[Ru(bpy)_2(bpSOp)](PF_6)_2$ in 1,2-dichloroethane at 490 nm.

References

1. A. W. King, Y. Jin, J. T. Engle, C. J. Ziegler, and J. J. Rack, *Inorg. Chem.*, 2012, **52**, 2086–2093.

2. J.-P. Collin, D. Jouvenot, M. Koizumi, and J.-P. Sauvage, *Inorganica Chim. Acta*, 2007, **360**, 923–930.

3. M. K. Smith, J. A. Gibson, C. G. Young, J. A. Broomhead, P. C. Junk, and F. R. Keene, *Eur. J. Inorg. Chem.*, 2000, 1365–1370.